HAL
open science

Greenland Sea sea ice variability over 1979-2007 and its link to the surface atmosphere

Agathe Germe, Marie-Noëlle Houssais, Christophe Herbaut, Christophe Cassou

To cite this version:

Agathe Germe, Marie-Noëlle Houssais, Christophe Herbaut, Christophe Cassou. Greenland Sea sea ice variability over 1979-2007 and its link to the surface atmosphere. Journal of Geophysical Research, 2011, 116, pp.10034. 10.1029/2011JC006960 . hal-00755090

HAL Id: hal-00755090

https://hal.science/hal-00755090v1

Submitted on 29 Oct 2021

HAL is a multi-disciplinary open access archive for the deposit and dissemination of scientific research documents, whether they are published or not. The documents may come from teaching and research institutions in France or abroad, or from public or private research centers.

L'archive ouverte pluridisciplinaire **HAL**, est destinée au dépôt et à la diffusion de documents scientifiques de niveau recherche, publiés ou non, émanant des établissements d'enseignement et de recherche français ou étrangers, des laboratoires publics ou privés.

Copyright

Greenland Sea sea ice variability over 1979–2007 and its link to the surface atmosphere

Agathe Germe,[1] Marie-Noëlle Houssais,[1] Christophe Herbaut,[1] and Christophe Cassou[2]

Received 13 January 2011; revised 20 July 2011; accepted 28 July 2011; published 28 October 2011.

[1] Mean winter Arctic sea ice concentration based on passive microwave observations for the period 1979–2007 are analyzed to examine the variability of the western Nordic Seas marginal ice zone (MIZ). A principal component analysis performed on this regional domain shows that the interannual variability is dominated by a mode which captures more than 70% of the total variance and shows only moderate correlation with the leading mode of global Northern Hemisphere sea ice variability. This mode appears to be related to a pattern of sea level pressure (SLP) anomaly centered on the MIZ with large scale signature resembling the canonical pattern of the North Atlantic Oscillation (NAO). Still this leading mode of SIC variability shows a weak temporal correlation with the NAO index. Taking into account the intrinsic spatial asymmetry found between the two phases of the NAO based on a weather regimes analysis, composite SIC fields are constructed which indeed suggest a preferential response of the Greenland Sea SIC variability to negative NAO-like patterns of SLP. The SLP pattern is consistent with a response of the sea ice margin to the strength of the northerly winds along eastern Greenland. A weak pattern of surface air temperature anomalies also emerges in the central Greenland Sea which occurs, at least partly, as a response of the surface atmosphere to sea ice concentrations changes. Higher order modes of winter SIC variability emerge based on a shorter winter season. One mode has much resemblance with the Odden/Nordbukta pattern while another one exhibits a significant signature in the center of the Greenland Sea convective gyre. The Odden/Nordbukta mode shows a more symmetric relation to the NAO than the leading SIC mode. Linear regression analysis consistently suggests some link between this mode and the ice area flux through Fram Strait.

Citation: Germe, A., M.-N. Houssais, C. Herbaut, and C. Cassou (2011), Greenland Sea sea ice variability over 1979–2007 and its link to the surface atmosphere, *J. Geophys. Res.*, *116*, C10034, doi:10.1029/2011JC006960.

1. Introduction

[2] Sea ice plays a crucial role in the energy balance of the climate system. Its insulating properties limit the heat and mass exchanges between the ocean and the atmosphere while its high albedo controls the amount of solar radiative energy absorbed at the earth surface. Particularly intense air-ice-sea interactions take place in the transition zones at the outer rim of the ice pack where strong spatial gradients of sea ice concentrations exist between the interior ice pack and the open ocean. In the Arctic, these marginal ice zones (MIZ), present in all peripheral seas (Figure 1), capture most of the seasonal and longer term sea ice variability.

[3] In the MIZ of the Atlantic and Pacific sectors, the winter sea ice cover is dominated by out-of-phase interannual fluctuations known as the Atlantic and the Pacific seesaws, which occur between the Labrador and Nordic Seas, and between the Okhotsk and the Bering Seas, respectively [*Walsh and Johnson*, 1979; *Cavalieri and Parkinson*, 1987; *Fang and Wallace*, 1994]. The leading mode of the Northern Hemisphere (NH) sea ice concentration (SIC) variability obtained from an Empirical Orthogonal Function (EOF) analysis over the last decades is indeed characterized by a double dipole pattern (accounting for about a third of the variance depending on the period and the definition of the winter season) consistent with the dipoles in the two ocean sectors being significantly correlated [*Mysak and Venegas*, 1998; *Deser et al.*, 2000; *Ukita et al.*, 2007].

[4] Superimposed to the large scale covariability of the NH sea ice, regional contrasts between the MIZ have been identified both over the historical period [*Mysak and Manak*, 1989] and over the more recent period of satellite observations [*Parkinson et al.*, 1999]. In the Greenland Sea (GS), a regional pattern of variability is a protrusion of sea ice, known as the Odden feature, which extends northeastward from the interior MIZ between about 71°N and 74°N, and covers an area of up to 3 10^5 km^2 [*Shuchman et al.*, 1998]. This feature, highly variable in time and space, captures a significant part of the large scale NH SIC variability as shown by the local maximum of SIC variance in the leading

[1]LOCEAN, UMR 7159, CNRS/UPMC/IRD/MNHN, Paris, France.
[2]Climate Modelling and Global Change Project, CNRS-CERFACS, Toulouse, France.

Copyright 2011 by the American Geophysical Union.
0148-0227/11/2011JC006960

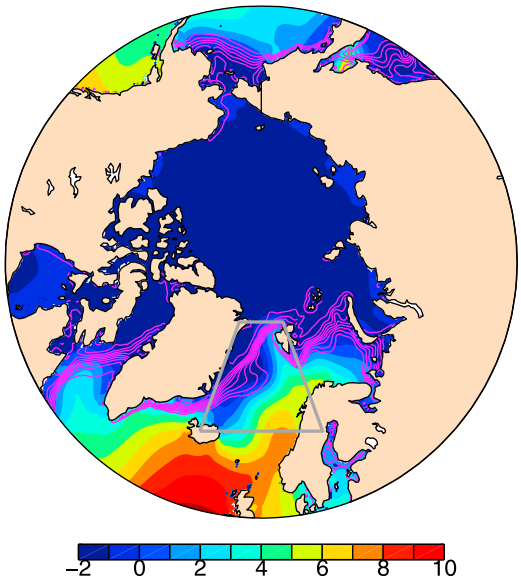

Figure 1. Climatology of the PHC3 (updated from *Steele et al.* [2001]) sea surface temperature (filled color contours) and SIC (magenta contours, contour interval is 0.1) in January. Also shown is the domain of study (gray box).

mode of the NH winter SIC variability or by the significant correlation (r = 0.64) between the time series of the Odden mean area and the principal component (PC) associated with this leading mode [*Deser et al.*, 2000]. Still, changes in the shape and location of the Odden may not be well represented in this large scale leading mode. These changes include eastward incursions of the Odden into the Greenland Gyre and occasional occurrences of the Nordbukta, an area with low ice concentration intruding into the northwest part of the Odden and leading to a tongue-like shape of the Odden [*Wadhams and Comiso*, 1999]. This complex pattern of variability of the Odden is not better reproduced in a rotated EOF analysis of the northern Atlantic/Arctic SIC variability [*Rogers and Hung*, 2008]. The PC associated with the second most important rotated EOF reproduces some of the major Odden events of the 1990s but the single center of variability retrieved in the GS bears little resemblance to the complex Odden/Nordbukta pattern.

[5] The large scale pattern of the NH SIC anomalies is to a large extent set by the atmosphere [*Fang and Wallace*, 1994; *Deser et al.*, 2000; *Partington et al.*, 2003]. In particular, the leading mode of the winter SIC was shown to correlate high (0.64) with the North Atlantic Oscillation (NAO) [*Deser et al.*, 2000]. As noticed by *Ukita et al.* [2007], this relationship may be largely dominated by the response of this leading mode in the Atlantic sector, which is the preferred domain of action of the NAO. This would be consistent with the higher correlation of the SIC PC1 with the NAO than with the AO [*Partington et al.*, 2003].

[6] As part of the Atlantic SIC dipole pattern, the GS MIZ is expected to be linked with the NAO, with reduced sea ice cover corresponding to periods of positive NAO index. Still, within this dipole, the GS seems to be the least responsive region to the NAO compared with the Labrador Sea or the Barents Sea [*Vinje*, 2001a]. In particular, the anticorrelation between the GS ice cover and the winter NAO does not appear to be very robust. A significant negative correlation (r = −0.60) is observed between the winter NAO and the GS ice extent over the period 1864–1996 [*Vinje*, 2001a], but the anticorrelation decreases when considering only the second part of the twentieth century [*Kvingedal*, 2005a] and even becomes positive after the early 70s [*Comiso et al.*, 2001; *Shuchman et al.*, 1998]. The correlation is also weak when the principal component of the second rotated EOF of the SIC is considered instead of the ice extent [*Rogers and Hung*, 2008]. The large spread of correlation values confirms that the mechanisms underlying the GS sea ice cover variability have a complex link to the atmosphere or are not exclusively driven by it.

[7] Several factors can be responsible for the specific behavior of the GS sea ice cover. In particular, it should be influenced by the ice efflux through Fram Strait, but the statistical relationship between the transport and the GS ice extent/area is still to be established. *Kern et al.* [2010] do mention significant positive correlation between the winter sea ice area flux through Fram Strait and the summer GS ice area over the period 1992–2008 but this relationship breaks down for the winter anomalies. This lack of correlation would be consistent with the fact that the GS sea ice cover does not show a robust link to the NAO despite the positive correlation between the NAO and the sea ice area flux through Fram Strait [*Kwok et al.*, 2004]. Alternatively, *Kern et al.* [2010] suggest that local sea ice formation is the main mechanism controlling the variability of the GS ice cover but their conclusion needs to be confirmed by a more systematic analysis.

[8] More generally, we lack knowledge of the mechanisms controlling the Odden variability. According to *Wadhams and Comiso* [1999], the Odden may appear as an early winter feature formed through local thermodynamic growth or as a late winter feature carrying old ice advected from the East Greenland Current (EGC). Yet, no link has been established between the spatial distribution of the Odden and its possible origins. *Shuchman et al.* [1998] and *Comiso et al.* [2001] all agree that, at the interannual time scale, the surface air temperature (SAT) controls to some extent the Odden variability. Their conclusions however diverge concerning the impact of the surface winds on the shorter term variability, in particular with regard to which wind direction should be the more conducive to Odden growth. It should be noted that both studies rely on analyses of Odden events of short duration which may not be entirely relevant for the interannual variability. Earlier analyses also agree that the ocean may exert a strong control on the Odden variability. This would be due to the proximity of the ice tongue to the surface oceanic front separating the Arctic Intermediate Water of the interior Greenland Gyre from the warm Atlantic water to the east (Figure 1) and modulating local melt and freezing, and to mechanical (currents, waves) effects. In particular, the GS MIZ coinciding with one of the major deep convection sites of the North Atlantic, the upward heat flux associated with convective mixing may be an important forcing at the bottom of the ice. These oceanic influences on the sea ice are still to be quantified and understood.

[9] In the present study, the interannual variability of the GS sea ice cover is analyzed with a focus on (1) describing the regional spatial modes of sea ice variability in the GS

over the period of satellite observations (1979–2007), and determining their relation to the Odden feature, and (2) identifying the contribution of the atmospheric forcing to the GS winter sea ice variability and revisiting the possible link to the NAO. We first describe in section 2 the observations used for the analysis as well as some methodological aspects. In section 3, the variability of the GS sea ice cover is presented based on spatially integrated indices. The spatial patterns of the sea ice concentration variability are calculated from a regional principal component analysis (PCA) in section 4 and their ability to represent the variability of the GS MIZ is discussed. In section 5 the relation to the atmospheric forcing is analyzed and section 6 is devoted to a discussion on the relationship to the NAO, in particular through the weather regime paradigm. Some conclusions are presented in section 7.

2. Data

2.1. Sea Ice Concentration Data

[10] We use sea ice concentrations [*Cavalieri et al.*, 1996] derived from brightness temperatures acquired by the Scanning Multichannel Microwave Radiometer (SMMR) over 1978–87 and the Special Sensor Microwave Imager (SSM/I) over 1987–2007. The data have been provided by the National Snow and Ice Data Center in a polar stereographic projection on a 25 km × 25 km grid (http://nsidc.org/data/polar_stereo/ps_grids.html). Despite their moderate spatial resolution, these observations offer the best coherent data set for investigating the space-time variability of the sea ice cover since 1978. The period selected for the analysis corresponds to the one for which quality controlled (as opposed to real time) data are available. Because of spacecraft power limitations, the SMMR concentrations are only available every other day while the SSM/I concentrations are sampled daily. In order to have a uniform data set, we linearly interpolate SMMR concentrations to daily values.

[11] We use sea ice concentrations calculated using the NASA Team (NT) algorithm [*Gloersen et al.*, 1984; *Cavalieri et al.*, 1984; *Gloersen and Cavalieri*, 1986]. The NT algorithm has been chosen for consistency reasons with the sea ice concentrations used in the atmospheric reanalyses (see below). While there are significant discrepancies in absolute concentration between the Bootstrap [*Comiso*, 1986] and the NT derived SIC, the time-space variability retrieved from an EOF decomposition over the entire Arctic domain is very similar between the two data sets [*Singarayer and Bamber*, 2003].

2.2. Atmospheric Data

[12] In order to investigate the link between the sea ice distribution and the atmosphere, daily atmospheric surface fields provided by the European Center for Medium-Range Weather Forecast (ECMWF) reanalyses are used. Outputs from the ERA-Interim reanalysis covering the recent period 1989–2007 [*Berrisford et al.*, 2009] are supplemented by the ERA-40 reanalysis [*Uppala et al.*, 2005] surface fields prior to 1989 back to 1978. The combined data set is hereafter referred as the ECMWF data set. As input to the present study, we use the sea level pressure (SLP), the 2-m air temperature, the 10-m zonal and meridional wind components as well as the surface sensible and latent heat flux and the net solar and thermal radiation fields. All fields are available on the ECMWF N80 quasi regular Gaussian grid which has equivalent spatial resolution of 1.125° (roughly 125 km and 35 km in the meridional and zonal direction, respectively).

[13] By construction, the reanalyzed atmospheric fields are dynamically adjusted to the prescribed surface fields used as boundary conditions for the atmospheric model. In both ERA40 and ERA-Interim these fields are constructed based on the same satellite derived SIC data as we are using for our analysis [*Reynolds et al.*, 2002] (http://polar.ncep.noaa.gov/sst/oper/Welcome.html). Comparison between the two SIC data sets in the GS MIZ shows that the sea ice extent derived from the satellite observations over the GS MIZ is indeed very similar to that deduced from the ECMWF SIC data set (not shown). The time space distribution of the SIC variability revealed by a PCA is also very similar between the two data sets (not shown). In particular, the detrended principal components associated with the first, second and third leading modes correlate high (0.94, 0.86 and 0.93, respectively).

3. Regional Indices of the Sea Ice Cover Variability in the Central Greenland Sea

3.1. Time Series of the Winter Sea Ice Area

[14] We are interested in the western sea ice margin of the Nordic Seas encompassing the GS and the western Icelandic Sea. Based on the mean winter (DJFMA) SIC distribution, two contrasted regions can be identified (Figure 2a); those are separated by a strong northwestward SIC gradient roughly corresponding to the front separating the EGC to the west from the interior Greenland Basin to the east [*Swift*, 1986]. The first region, coinciding more or less with the East Greenland shelf, is characterized by a compact (concentration larger than 50%) sea ice cover and a weak year-to-year variability. The second region (hereafter referred to as the MIZ), extending eastward from the East Greenland shelf-slope region, is covered by less compact ice and shows much larger variance (standard deviation of the winter SIC can reach same order as the long-term mean in the gyre interior) (Figure 2b).

[15] In order to define a mean index of sea ice variability, spatially averaged properties have been calculated over the region of enhanced SIC variability, delimited by the thick line in Figure 2, which roughly corresponds to the MIZ region. Since sea ice concentrations are low in summer we chose to focus our analysis on the winter season that is found to largely dominate the mean annual SIC variability. The winter season (DJFMA) is however chosen wide enough to encompass the year to year contrasts in the duration and timing of the ice season.

[16] Over 1979–2007, the DJFMA sea ice area in the GS MIZ shows a strong downward trend of 4.5% per year explaining 28% of the variance (Figure 3a). There is a large interannual variability around that trend with standard deviation reaching 4.6 10^4 km^2, therefore having same order of magnitude as the mean (7.5 10^4 km^2) in agreement with the pattern in Figure 2b. The autocorrelation of the sea ice area indicates no year-to-year persistence. A spectrum analysis (not shown) reveals no significant peak in the interannual frequency band, in particular no peaks at periods of 2 and 4 years such as those observed by *Gloersen* [1995] when the full Arctic domain is considered. Decadal oscillations such as those reported by *Kvingedal* [2005b] and *Comiso*

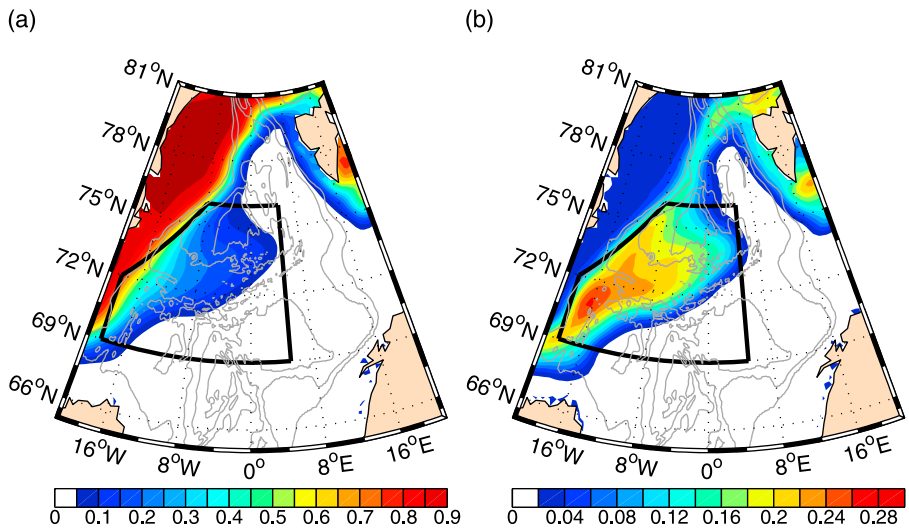

Figure 2. (a) Mean winter (DJFMA) sea ice concentration averaged over the 1979–2007 period and (b) standard deviation of the mean winter sea ice concentration over the 1979–2007 period. Also shown are the limits of the MIZ region (solid black box) and the 1000 m, 2000 m, 3000 m and 3500 m bathymetric contours (solid gray contours).

et al. [2001] for the Odden cannot be identified due to the too short period.

[17] Depending on the year, the mean winter SIC distribution exhibits Odden-like features with very different shapes. Contrasted distributions of the Odden/Nordbukta feature leading to tongue-like or bulge Oddens [*Wadhams and Comiso*, 1999] may however have similar signatures in the average sea ice area of the region, as shown by comparing for instance years 1987 and 1997 in Figures 3a and 4. There is therefore a need to take into account in a more systematic way the spatial and temporal evolution of the SIC distribution within the MIZ.

3.2. The Odden/Nordbukta Mode

[18] Subjective examination of the winter averaged SIC distributions for each individual year suggests that the appearance of the Odden/Nordbukta pattern, or alternatively of a bulge Odden, may be an adequate criterion to describe the year-to-year contrasts, at least during years of sufficient ice coverage. In order to characterize this variability, we therefore define the Nordbukta index based on the difference between the SIC characterizing the region at the extremity of the Odden (4.5°–3°W, 72.8°–73.5°N) and that of a region in the vicinity of the Nordbukta (8°–6.8°W, 74.3°–75.1°N). A positive phase of this index indicates that the ice concentration in the Nordbukta is smaller than in the Odden, implying the existence of a Nordbukta. A negative phase indicates that higher ice concentrations are found in the Nordbukta than in the Odden meaning that the Nordbukta is filled with ice. We interpret the latter case as a bulge-like Odden. The time series of the index is shown in Figure 3b. Except for years with a Nordbukta index close to zero corresponding to years with very small ice coverage, the index discriminates fairly well winters with an Odden/Nordbukta-like mean SIC distribution from winters with a bulge Odden-like distribution. As can be judged from Figures 3a and 3b, the Nordbukta index is weakly correlated with the mean winter sea ice area (correlation ~0.26) indicating that the Odden/Nordbukta feature has its own time variability which differs from that of the spatially averaged ice cover.

4. Leading Modes of Interannual Winter SIC Variability

[19] In order to describe the regional variability of the GS winter sea ice cover, a PCA is performed on the winter

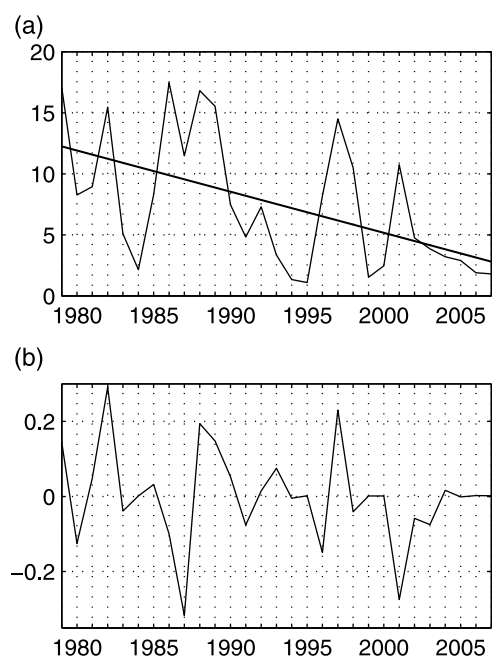

Figure 3. (a) Mean winter (DJFMA) sea ice area (in 10^4 km^2) calculated over the MIZ region and its linear trend over the period 1979–2007. (b) The Nordbukta index based on the mean winter (DJFMA) sea ice concentration difference between the Odden and the Nordbukta regions (see explanation in text). The correlation between the two time series is 0.26 (not significant at the 95% confidence level).

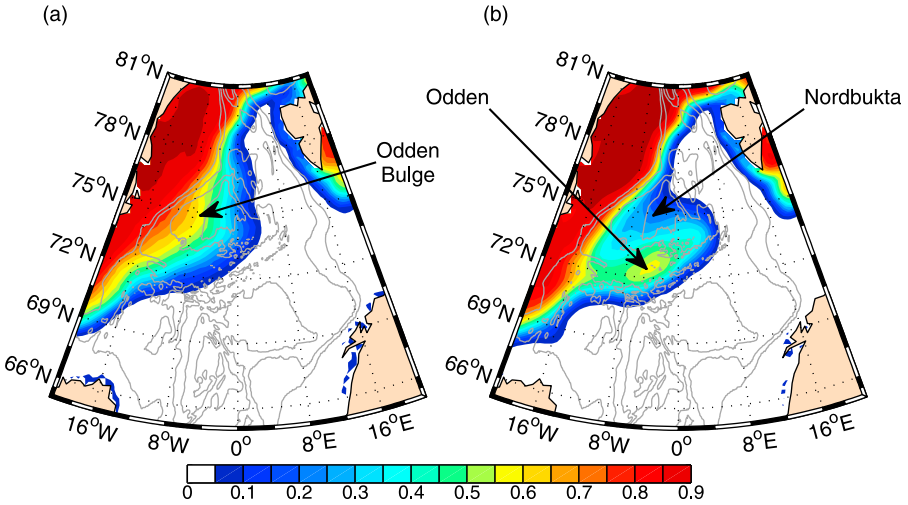

Figure 4. Mean winter (DJFMA) sea ice concentration in (a) 1987 and (b) 1997.

(DJFMA) SIC anomalies (obtained as departure from the 1979–2007 average) on a restricted geographical domain centered on the GS and extending from 68° to 81°N and from 21°W to 10°E (Figure 5). The domain includes the EGC area as well as the MIZ but excludes the marginal zone around Svalbard which is thought to have other sources of variability. While the PCA is performed on the raw SIC time series, all correlations are calculated with detrended time series.

[20] The leading mode of the SIC anomalies in the GS which accounts for 73% of the total variance exhibits a single pole covering the entire MIZ (Figure 5a) and showing much resemblance with the distribution of the standard deviation shown in Figure 2b. The maximum of the variability is found around 71–72°N and 16°W and is representative of the degree of eastward expansion of the ice cover in the form of an Odden feature. The associated time

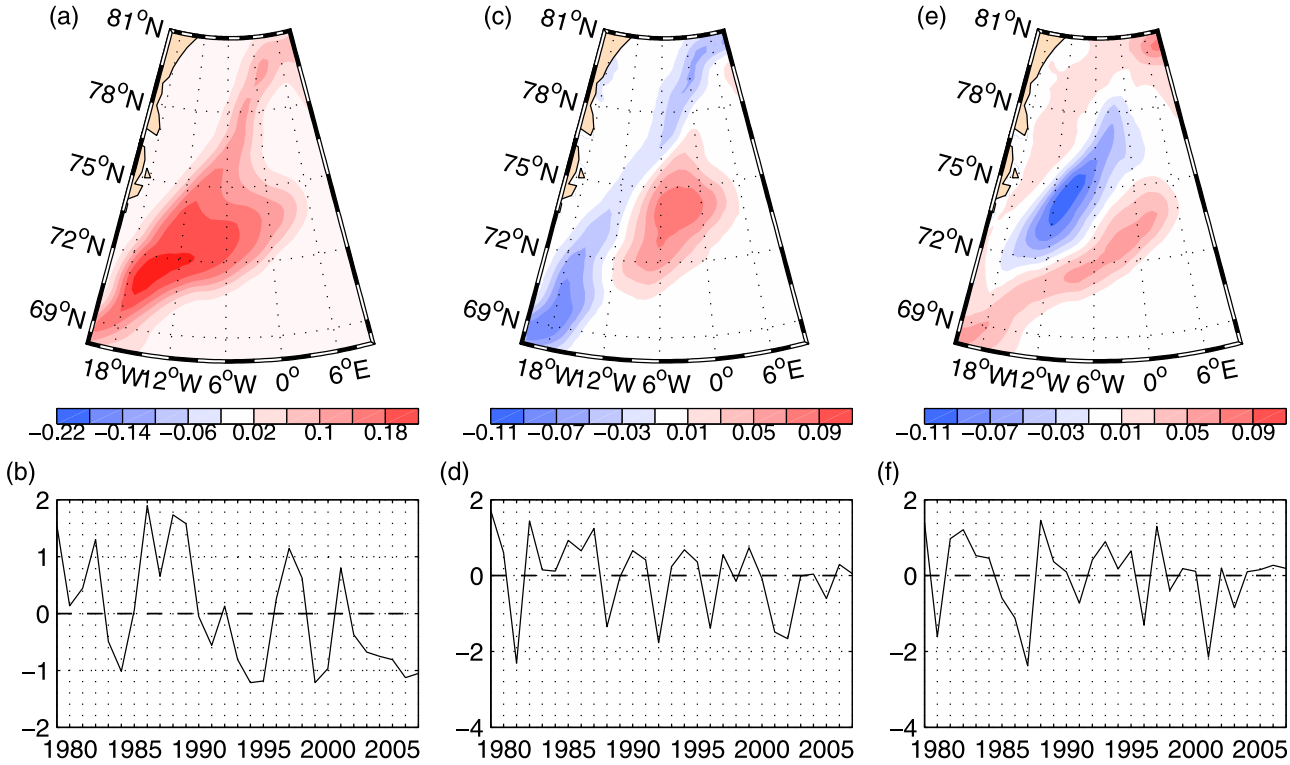

Figure 5. (top) Spatial patterns (EOF) and (bottom) principal component (PC) time series of the (a and b) first, (c and d) second and (e and f) third leading mode of the mean winter (DJFMA) sea ice concentration over 1979–2007. The first, second and third modes explain 73%, 8.1% and 7.3% of the total variance, respectively. In Figure 5 (top), ice concentration anomalies are expressed per unit standard deviation of the corresponding PC. The PCA is performed on the domain of the figure.

Table 1. In-Phase Correlation Between the Nordbukta Index and Each of the Three Leading Modes of the Mean Winter SIC in the GS[a]

	SIC PC1	SIC PC2	SIC PC3
Nordbukta index	0.22	0.16	**0.86**

[a]All time series are linearly detrended. Bold numbers indicate significant correlations (at the 95% level of confidence).

series (PC) exhibits a dominant time scale of a few years superimposed on a significant downward trend which were both identified in the time series of the sea ice area calculated over the MIZ box (Figure 3a). Once detrended, the two time series are indeed highly correlated (r = 0.96). Note that the leading GS mode is moderately correlated (r = 0.47) with the leading mode of Arctic sea ice variability (not shown) suggesting that the regional GS variability has its own dynamics.

[21] The two following modes of SIC variability altogether account for 16% of the variance (Figures 5c and 5e). According to the rule of thumb described by *North et al.* [1982], their respective eigen values are too close to each other for these two modes to be separable as they may just be a random mixture of true eigenvectors. Despite these limitations, it is interesting to note that the two corresponding EOF patterns can be paralleled with known patterns of the GS SIC variability. The second EOF extracts a dipolar structure. The pole in the outer MIZ is located roughly at the center of the GS convective area (74.5°N, 4°W). The PC associated with this EOF shows a weak (insignificant) trend but a large interannual variability. The third EOF presents a dipolar structure opposing SIC anomalies located around 72–74°N/6°W-0° to anomalies located around 74–76°N/12–6°W. The dipole is reminiscent of the Odden/Nordbukta feature. This resemblance suggests that, despite possible degenerescence between EOF2 and EOF3, some physical interpretation can be given to the EOF decomposition. The Nordbukta index is indeed strongly correlated with the PC of this third mode while it shows no significant correlation with the two other leading modes (Table 1). According to the extreme negative and positive values of the third PC, years 1979, 1981, 1982, 1988 and 1997 should be representative of a positive phase (enhanced dipolar pattern with deepened Nordbukta) and years 1980, 1986, 1987, 1996 and 2001 of a negative phase (weakened dipole associated with filled Nordbukta). The contrasted sea ice distributions between these two sets of years indeed allow us to discriminate remarkably well between the tongue-like Odden coupled to the Nordbukta feature (Figure 6, left) and the bulge-like Odden (Figure 6, right), respectively. However, the discrimination is less convincing at low values of the PC3 which correspond to cases where a subjective identification of the Nordbukta is also difficult (e.g., years 1989 and 1998, not shown). This mode also fails to identify years marked by a clear Odden/Nordbukta pattern but involving weak winter mean sea ice concentrations. Interestingly, such cases which contribute little to the interannual variability of the Odden/Nordbukta yet appear to be characterized by a strong intraseasonal variability within the winter season.

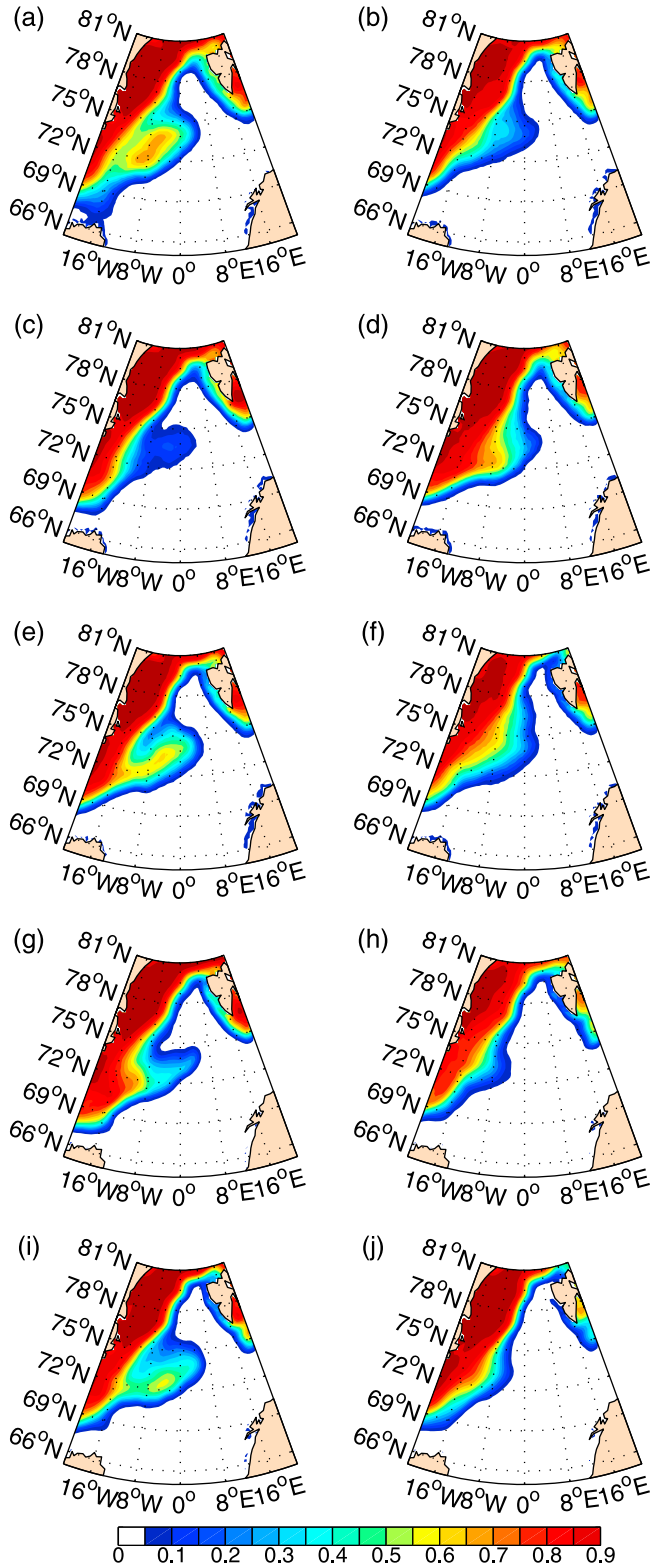

Figure 6. Mean winter (DJFMA) sea ice concentration in (a) 1979, (b) 1980, (c) 1981, (d) 1986, (e) 1982, (f) 1987, (g) 1988, (h) 1996, (i) 1997 and (j) 2001. Years with extreme (left) positive and (right) negative values of the third PC of the mean winter sea ice concentration (Figure 5f) are shown.

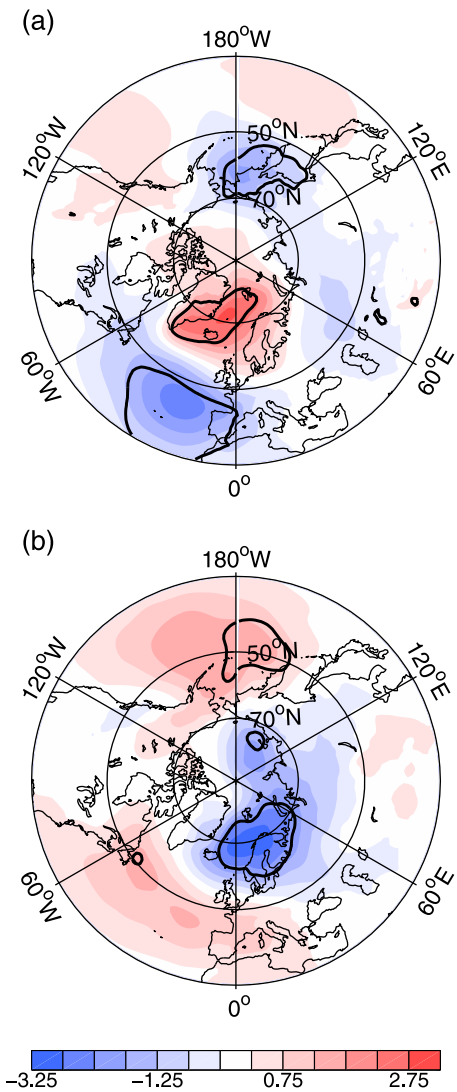

Figure 7. Linear regression of the mean winter (DJF) sea level pressure (in hPa) on the detrended (a) first and (b) third principal component of the mean winter sea ice concentration in the Greenland Sea, over the period 1979–2007. The black contour delimits the area where the regression is significant at the 95% level of confidence.

[22] Separate PCAs performed on monthly mean SIC anomalies for each winter month lead in all months except April to three distinct (according to the rule of thumb) leading modes of variability, with patterns very similar to those recovered from the PCA of the winter-averaged SIC anomalies. This suggests that all three leading modes are major modes of interannual variability of the monthly GS SIC during the DJFM winter period while the variability in transition periods like April would not be as well captured by these modes. For all winter months, the time series of the leading modes of the monthly SIC anomalies correlate high (at least 0.7) with the time series of the corresponding leading modes of the winter-averaged anomalies. Higher sensitivity to the selected month is found for the higher order modes (mode 2 and 3), which is interpreted as a signature of the intraseasonal variability characterizing these modes. The conclusion is consistent with the strong intraseasonal variability of the Odden/Nordbukta feature mentioned by *Wadhams et al.* [1996] or *Shuchman et al.* [1998].

5. Influence of the Surface Atmospheric Variability on the GS Winter SIC

[23] In order to determine which patterns of surface atmospheric circulation anomalies are linked to the winter GS SIC variability, a regression analysis of surface atmospheric fields on the leading mode of SIC variability has been performed. Daily surface atmospheric fields from the ECMWF reanalyses (see section 2.2) are used which are then averaged over the DJF period to form winter averaged fields. A two-sided Student's t-test is used to assess the statistical significance of the correlations between atmospheric and SIC time series. In view of the short decorrelation time scale of the SIC PC time series (the autocorrelations of the time series are insignificant at 1 year lag), annual values are considered independent from each other. The significance of the regressions is determined based on a 95% level of confidence. In the following, all regressions and correlations are calculated with detrended time series.

5.1. The Atmospheric Surface Circulation and the Leading Mode of SIC Variability

[24] Regression of the winter SLP anomalies on the GS SIC PC1 shows that a positive SIC anomaly is associated with a SLP dipole made of a positive anomaly over Iceland and a negative one over the Azores (Figure 7a) that resembles the NAO pattern (see discussion in section 6). Regressed surface wind anomalies corresponding to this SLP pattern (Figure 8b) show an anticyclonic circulation anomaly around Iceland associated with high ice cover in the GS leading to southerly wind anomalies along eastern Greenland or, equivalently, to a reduction of the mean northerly winds (Figure 8a). The resulting Ekman drift should lead to a reduction of the westward component of the ice drift, therefore making easier expansion of the sea ice into the interior GS.

[25] We also expect an impact of the reduced northerly winds along eastern Greenland on the ice import through Fram Strait. The pattern of SLP anomalies shown in Figure 7a indeed exhibits a strong cross-strait gradient anomaly in the Fram Strait which, in scenarios of enhanced sea ice cover, should act to reduce the ice efflux from the Arctic Ocean to the GS [*Vinje*, 2001b; *Tsukernik et al.*, 2009]. The expected impact would be that less ice be driven into the GS, leading to a negative SIC anomaly in contrast to what is observed. However, over 1979–2007, close-to-zero correlations are found between the SIC PC1 and the winter (October through May) or the annual ice area flux (IAF) given by *Kwok* [2009] (Table 2). This absence of correlation confirms that, at the interannual time scale, the IAF through Fram Strait does not exert a strong control on the GS winter SIC variability and that other driving mechanisms must prevail.

5.2. The Surface Air Temperature and the Leading Mode of SIC Variability

[26] The linear regression of the winter SAT on the SIC-PC1 exhibits a large scale dipole pattern associating a positive SIC anomaly in the GS to warm air anomalies over the Labrador Sea and southern Greenland and cold air anomalies

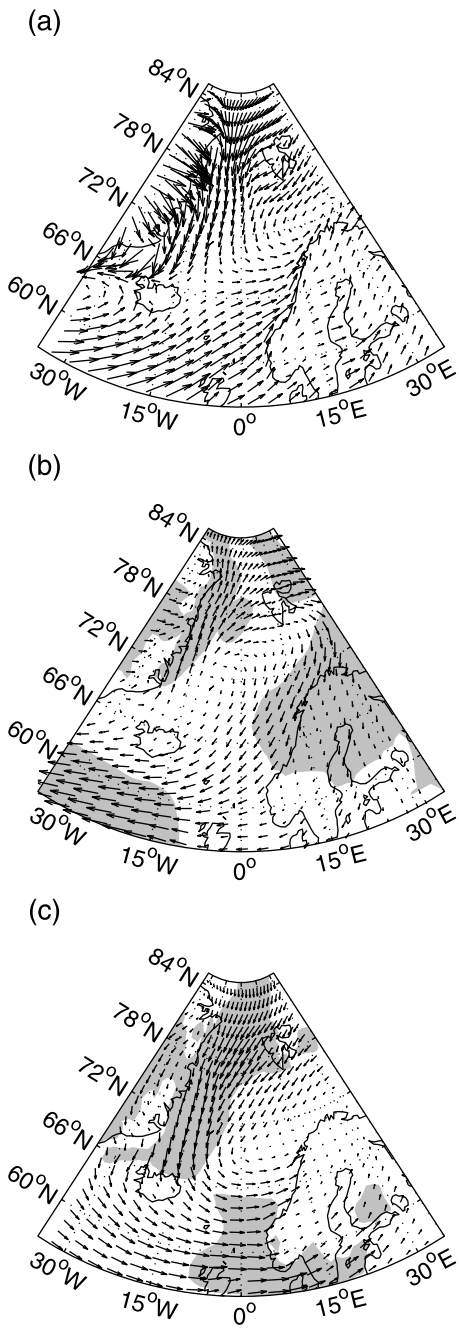

Figure 8. Mean winter (DJF) 10-m winds (a) averaged over the 1979–2007 period, (b) linearly regressed on the detrended GS SIC PC1 and (c) linearly regressed on the detrended GS SIC PC3, over the period 1979–2007. The gray shading delimits the area where the regression is significant at the 95% level of confidence. For Figures 8b and 8c, a separate regression is performed for each of the wind components and the significance is determined based on the condition that at least one regressed component is significant.

over a large region covering the Nordic Seas with enhanced signature over the Barents Sea and GS MIZ (Figure 9a). The wind curl anomaly in relation to the leading mode of SIC variability (Figure 8b) links the northerly wind anomalies along eastern Greenland to the anomalous westerlies over the Norwegian Sea. The mean northerly winds prevailing along eastern Greenland modulate cold air advection from the Arctic to the GS while the strength of the westerlies prevailing over the Norwegian Sea controls the advection of warm air from the Atlantic. Being located at the center of the wind curl anomaly, the GS MIZ is expected to feel the contradictory influences of these two processes. If one hypothesizes that large scale heat advection is responsible for the SAT anomalies, the pattern would suggest that the effect of reduced westerlies dominates over the effect of reduced northerlies.

[27] Another possible scenario could be that part of the anticorrelation between the winter SAT and the winter SIC in the GS be the result of the positive feedback of the sea ice cover onto the lower atmosphere. Such a feedback has been suggested by *Deser et al.* [2000] in relation to the leading mode of the Arctic sea ice variability. Enhanced sea ice cover acting as an insulator puts less of the ocean surface in direct contact with the atmosphere and therefore reduces the atmosphere surface warming leading to negative SAT anomalies. Examination of the air-ice/sea heat flux anomalies associated with the winter SIC variability (Figure 10a) reveals that enhanced SIC in the GS is associated with a downward heat flux anomaly suggesting that a sea ice-atmosphere heat flux feedback is indeed at work and dominates over the direct action of the SAT on the sea ice. Compared with the GS MIZ, in the Barents Sea region, the heat flux anomalies are of opposite sign despite SAT, as well as SIC anomalies as part of the Atlantic seesaw, have the same sign. This suggests that surface air temperature anomalies in the Barents Sea control to some extent the SIC distribution with a lesser impact of the surface heat flux feedback. This is in agreement with the dominance of the westerlies in this region (Figure 8a) and their ability to drive anomalies of air temperature advection that further imprints SIC anomalies.

5.3. Atmospheric Forcing on the Odden/Nordbukta Mode

[28] Regression of winter SLP on the SIC PC3 (Figure 7b), taken here as a proxy of the Odden/Nordbukta mode, shows a pole of significant negative SLP anomalies centered on the Norwegian-Barents Sea region. Compared with the SLP regression on the SIC PC1, the pole of action is significantly shifted to the northeast. During periods of enhanced Odden/Nordbukta pattern (positive value of the PC), these SLP anomalies appear to be associated with a wide pattern of southwestward surface wind anomalies over the GS MIZ (Figure 8c) which should favor a westward sea ice retreat.

Table 2. In-Phase Correlation Between the Principal Components of the Three Leading Modes of the Mean Winter Sea Ice Concentration and Indices of Atmospheric Variability, Oceanic Variability, or Sea Ice Area Flux Through Fram Strait[a]

	NAO	Winter IAF	Annual IAF	Convection Depth
GS SIC PC1	**−0.41**	0.06	−0.02	0.24
GS SIC PC2	−0.19	−0.31	−0.21	**−0.48**
GS SIC PC3	0.36	**0.50**	**0.46**	−0.29

[a]Atmospheric variability, winter NAO index; oceanic variability, Greenland Sea winter convection depth from *Budéus and Ronski* [2009]; sea ice area flux (IAF) through Fram Strait, from *Kwok* [2009]. All time series are linearly detrended. See explanations in text for the index definitions. Bold numbers indicate significant correlations (at the 95% level of confidence).

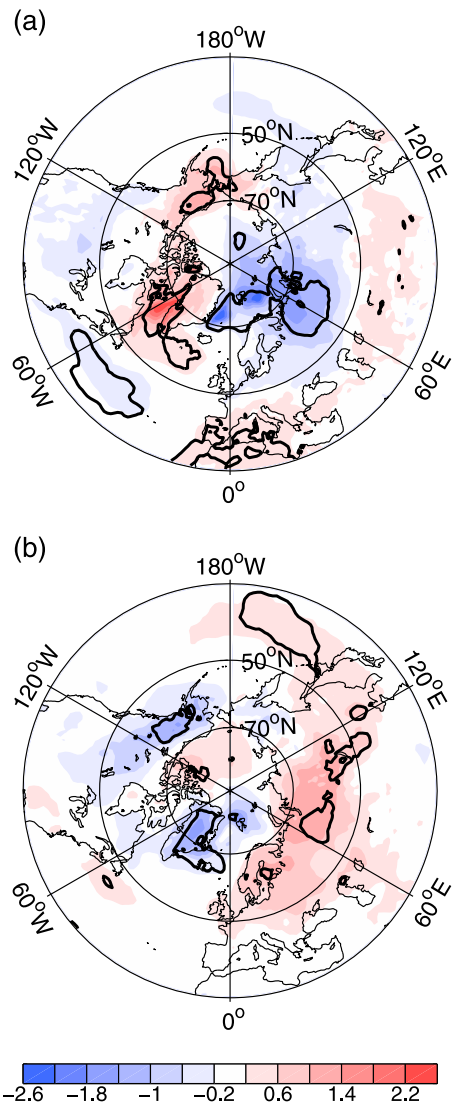

Figure 9. Linear regression of the mean winter (DJF) surface air temperature (in °C) on the detrended (a) first and (b) third principal component of the mean winter sea ice concentration in the Greenland Sea, over the period 1979–2007. The black contour delimits the area where the regression is significant at the 95% level of confidence.

There is therefore no evidence that the direct action of this wind anomaly pattern on the GS MIZ could drive an enhanced Odden/Nordbukta pattern.

[29] In relation to the SIC PC3, significant wind anomalies are found in Fram Strait (Figure 8c). These anomalies are associated with a cross-strait SLP gradient which has opposite sign to the gradient associated with the SIC PC1 and, in scenarios of enhanced Odden/Nordbukta pattern, should be conducive of an increase of the ice import to the GS. The SIC PC3 indeed positively correlates with both the winter and the annual IAF through Fram Strait (r = 0.50 and 0.46, respectively), and the linear regression pattern of the winter SIC on the winter IAF (not shown), though not significant in the MIZ region, shows a dipolar pattern strikingly similar to the EOF3. Therefore, the northerly winds through Fram Strait, and consequently the import of arctic sea ice to the GS, seem to be more connected with the spatial redistribution of the sea ice anomalies within the GS than with the overall extent of the sea ice cover. Reasons for this link still need to be elucidated.

[30] Although no significant SAT anomalies are found in relation to the third mode of GS SIC anomalies (Figure 9b), significant surface heat flux anomalies are found in the Nordbukta region (Figure 10b). As for the first leading mode of SIC variability, the sign of the flux (a heat loss for the ocean in relation to an opening of the Nordbukta) indicates a feedback of the ice onto the atmosphere. Lack of associated positive SAT anomalies however suggests that other processes should control the temperature of the atmospheric boundary layer in this region.

6. Link With Modes of Surface Atmospheric Variability

6.1. Link With the NAO

[31] Table 2 sums up the correlation of the PCs of the three leading SIC modes with the NAO index. The NAO is

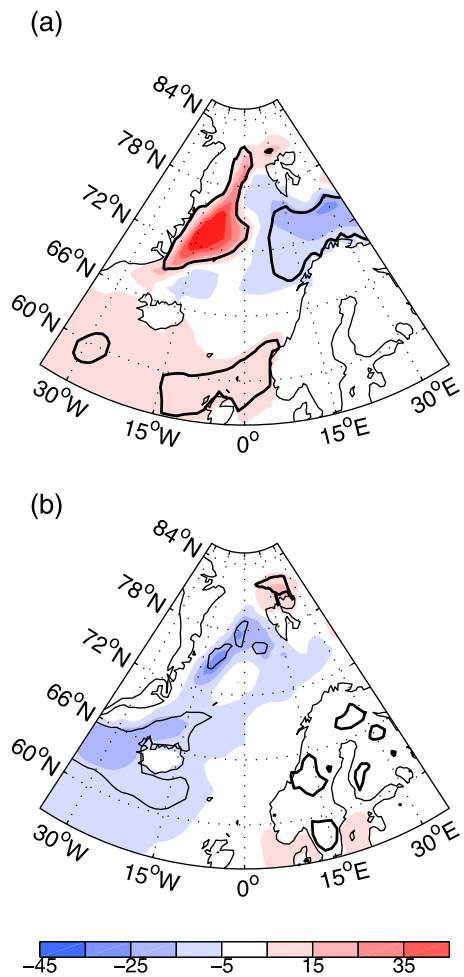

Figure 10. Linear regression of the mean winter (DJF) surface heat flux (in W m^{-2}) on the detrended (a) first and (b) third principal component of the mean winter sea ice concentration in the Greenland Sea, over the period 1979–2007. The black contour delimits the area where the regression is significant at the 95% level of confidence. Positive values indicate a downward flux.

defined as the PC associated with the leading mode of the winter (DJF) SLP calculated over the Atlantic domain (20°N–81°N and 80°W–60°E, Figure 11a) [*Hurrell et al.*, 2003]. Note that correlations greater than 0.36 are significant at the 95% level of confidence. The NAO index only shows a weak anticorrelation (r = −0.41) with the leading mode of the GS SIC variability. Yet, the SLP pattern shown in Figure 7a resembles the NAO pattern except for a southwestward shift of its northern center of action toward Greenland compared to the canonical NAO pattern obtained from the PCA.

[32] The correlation of the NAO with the SIC PC3 is positive but barely significant. This is consistent with the fact that the southern center of action of the NAO in the North Atlantic is only weakly captured by the SLP regression although being of the correct sign (Figure 7b). In the Nordic Seas, the SLP regression shows however a pole that is very similar to the northern center of action of the NAO. The latter being recognized as an essential driver of the ice efflux through Fram Strait [*Kwok and Rothrock*, 1999; *Kwok et al.*, 2004], the similarity between the two patterns in this region may explain the significant correlation of the PC3 with the ice area flux through Fram Strait (Table 2). It also suggests that the mechanisms controlling the sea ice Odden/Nordbukta variability may have some relationship to the NAO via Fram Strait.

6.2. Link With North Atlantic Weather Patterns

[33] As highlighted in the previous section, the SLP regression in Figure 7a shows an anomalous pole centered in the Icelandic-Greenland Sea which is shifted compared to the canonical NAO pattern shown in Figure 11a. The shift may just express the continuous evolution of the NAO pattern over the recent period with a southwestern position of the pole being more representative of a link of the sea ice to the atmosphere during the earlier years of our period of investigation [*Zhang et al.*, 2008]. Alternatively, in the context of the nonlinear description of the atmospheric variability through the identification of so-called weather regimes [e.g., *Reinhold and Pierrehumbert*, 1982; *Vautard*, 1990], the regressed pattern can be interpreted as typical for the negative phase of the NAO, while being much less representative of the NAO^+. The distinction between the two regimes relies on the existence of intrinsic spatial asymmetry between the two phases of the NAO as shown by *Cassou et al.* [2004] for the period 1950–2001. In order to further investigate the link between these weather regimes and the SIC variability, *Cassou*'s [2008] methodology is applied to the daily SLP data over 1979–2007 which leads to identify four SLP regimes: the NAO^+, NAO^-, Atlantic Ridge (AR) and Scandinavian blocking (S-BL) regimes. Because the dynamics are essentially barotropic, these regimes are very much similar to those obtained from geopotential height anomalies by *Michelangeli et al.* [1995] or *Cassou* [2008]. In particular, the spatial asymmetry between the two NAO regimes is well preserved and is mainly

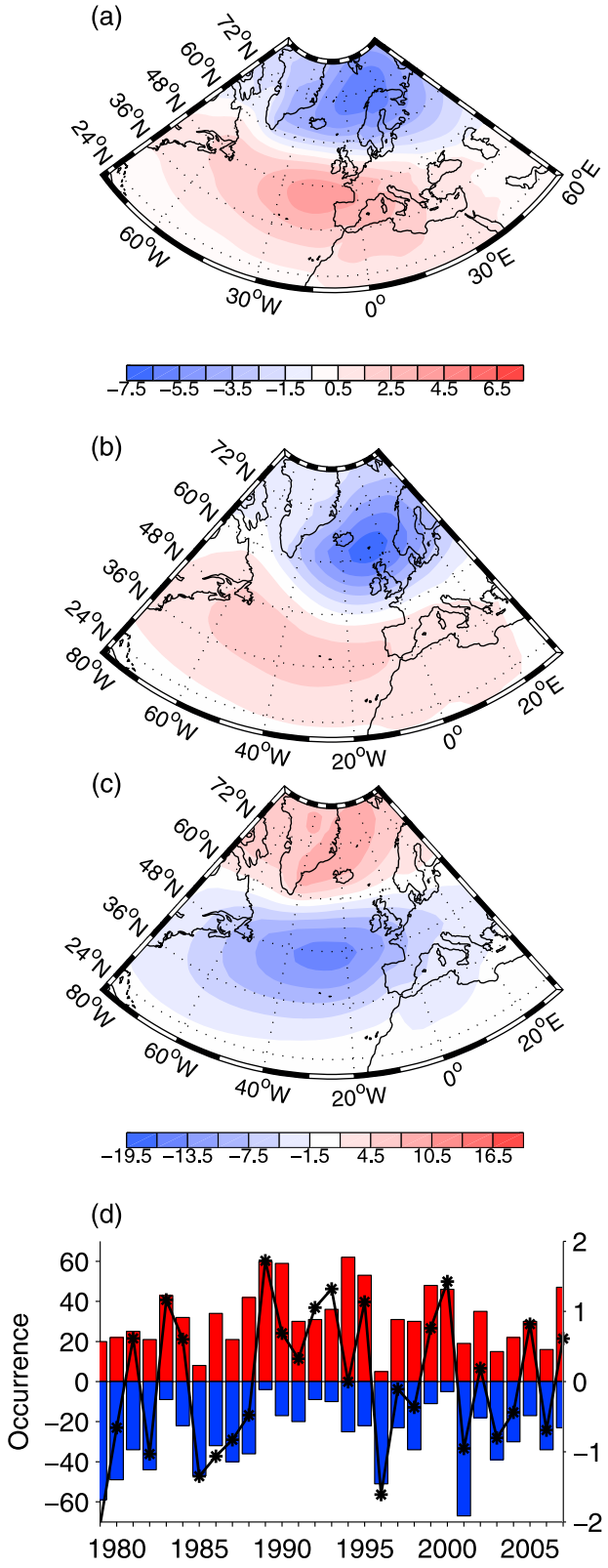

Figure 11. (a) Leading EOF (in hPa) of the winter (DJF) sea level pressure over the period 1979–2007 calculated over the Atlantic domain. This mode accounts for 50.4% of the total variance: patterns of (b) NAO^+ regime and (c) NAO^- regime based on daily averaged sea level pressure (in hPa) from the NCEP/NCAR reanalysis. (d) Time series of occurrence (in days) of the NAO^+ (red bars) and NAO^- (blue bars) regimes. Also shown in Figure 11d as a solid black line is the winter NAO index (the PC associated with the EOF shown in Figure 11a).

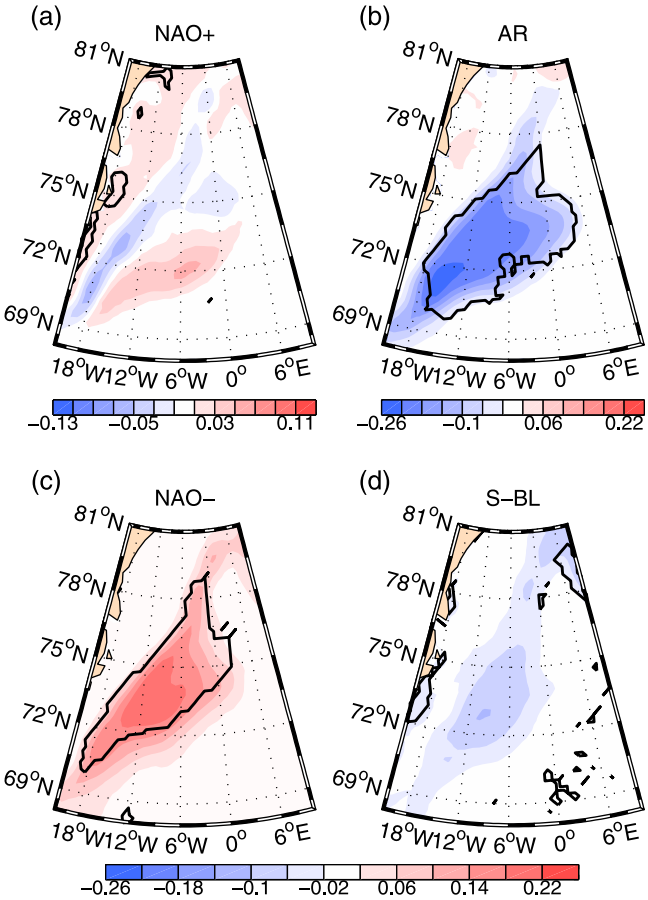

Figure 12. Composites of the mean winter (DJFM) sea ice concentration for each of the four North Atlantic weather regimes: (a) NAO$^+$, (b) AR, (c) NAO$^-$ and (d) S-BL. Composites are based on years when the regime dominates over the other three regimes. Composite years are: (a) 1983, 1986, 1988, 1989, 1990, 1994, 1995, 1999 and 2007; (b) 1984, 2000, 2004 and 2005; (c) 1979, 1980, 1981, 1982, 1987, 1996, 1998 and 2001; and (d) 1985, 1991, 1992, 1993, 1997, 2002, 2003 and 2006. The black contour delimits the area where the composite is significant at the 95% level of confidence.

characterized by the eastward shift of the northern center of action in NAO$^+$ compared to NAO$^-$ where maximum anomalies are found immediately on the eastern side of Greenland (Figures 11b and 11c). Winter occurrences defined as the number of days during DJFM for which a given regime is excited show that, despite both the NAO$^+$ and NAO$^-$ series individually correlate with the NAO index, each of the two series shows differences with the NAO and between each other (Figure 11d).

[34] Considering the distinct spatial patterns of the two phases of the NAO, it is likely that the weak correlation of the GS winter SIC PC1 with the NAO index expresses the preferential link of the GS SIC to the NAO$^-$ regime, NAO$^+$ dynamics being not that discriminant for the evolution of the whole GS as captured by EOF1. In order to check this hypothesis, we construct anomalous composite of the GS winter SIC based on the series of winter occurrences of the four atmospheric regimes. Each winter is associated with a single "climatic regime" defined as the dominant (in terms of number of occurrences) weather regime over DJFM. Four composites of the GS winter SIC are then calculated corresponding to the four climate regimes. In Figure 12c a strong response of the GS winter SIC is identified associated with the NAO$^-$ regime. The pattern resembles closely that of the leading EOF of the GS SIC. By contrast a similar, opposite sign pattern is not retrieved for the NAO$^+$ winters (Figure 12a) being instead associated with the AR regime (Figure 12b). Obviously such symmetry cannot be represented by a linear relationship to the NAO index, which explains why the correlation is weak with the latter. Note that even though strong negative SIC anomalies are associated with the AR regime, the actual impact of this regime on the SIC variability over 1979–2007 may be weak in view of the small number of AR winters (only 4) identified over the period. A dipolar pattern of SIC variability appears in the GS MIZ in relation to the NAO$^+$ regime but it is not significant (Figure 12a). Note though that the resemblance of the composite with the Odden/Nordbukta feature (Figure 5e) is consistent with the SLP pattern in Figure 7b having the same pattern as the PCA-based NAO pattern over the Nordic Seas. It is also consistent with similar levels of correlation of the SIC PC3 with the series of occurrence of the NAO$^+$ and NAO$^-$ regimes (0.36 and −0.42 respectively). These results suggest that the Odden/Nordbukta response to the NAO would be somehow more symmetric. Projecting the winter SLP anomalies onto the regression pattern shown in Figure 7b (over the domain 55–85°N, 35°W-35°E) leads to a SLP index which can be correlated with the series of occurrence of the NAO$^+$ and NAO$^-$ weather regimes to check the degree of linearity of the Odden/Nordbukta response to the NAO. Similar levels of correlation of this index are found with the two regimes (−0.65 for NAO$^-$ and 0.66 for NAO$^+$, Table 3). By contrast, the levels of correlation are asymmetric for the SIC PC1 (0.72 for NAO$^-$ and −0.30 for NAO$^+$).

7. Discussion and Conclusions

[35] A regional PCA has been performed on the winter averaged (DJFMA) SIC in the Greenland Sea to identify the dominant patterns of variability. The leading mode is characterized by a single pole covering the entire GS. Although the regional PCA does not allow identifying unambiguously higher order modes of variability due to degenerescense, the third mode has a pattern very similar to the Odden/Nordbukta feature and its associated PC strongly

Table 3. In-Phase Correlation Between the First and Third Leading Modes of the Mean Winter Sea Ice Concentration in the Greenland Sea and of the SLP Index Associated With Each of These Modes, and the Time Series of Occurrence of the NAO$^+$ and NAO$^-$ Regimes[a]

	NAO$^+$	NAO$^-$
GS SIC PC1	−0.19	0.36
GS SIC PC3	0.37	**−0.42**
SLP index PC1	−0.30	**0.72**
SLP index PC3	**0.66**	**−0.65**

[a]Bold numbers indicate significant correlations (at the 95% level of confidence).

correlates (0.86) with the Nordbukta index based on the winter SIC gradient between the Nordbukta and the Odden Tongue. The degenerescence is removed when the SIC anomalies are considered on shorter (here monthly) time scales, meaning that the intraseasonal (from a few days to a few months) variability largely contributes to these modes. The Odden is indeed known to have a large daily variability in relation to the atmospheric synoptic variability [*Wadhams et al.*, 1996; *Shuchman et al.*, 1998; *Comiso et al.*, 2001]. Unlike the interannual variability that is clearly dominated by the duration of occurrence of the Odden independently of its precise shape, the intraseasonal variability is expected to emphasize the variability of the shape of the Odden and of the occurrence of the Nordbukta and therefore to project on higher order modes with smaller spatial scales.

[36] The pattern of the leading mode of the global Arctic SIC is regionally very similar to the leading mode of the GS winter SIC and their corresponding time series are significantly correlated (r = 0.47). This result indicates that the GS MIZ variability is to some extent linked with large scale processes which impact the whole Arctic. This is in agreement with *Ukita et al.* [2007] who showed that the leading mode of Arctic sea ice variability is dominated by the variability in the Atlantic sector. Still, the correlation between the regional and global leading modes is not that high, especially in comparison with the correlation between the Atlantic and the global Arctic leading mode (r = 0.79). Subtle differences must therefore exist between the GS and the Arctic SIC modes that we interpret as being linked to specific response to the regional atmospheric (and oceanic) forcing on the sea ice.

[37] The strongest correlations of SLP anomalies with the leading regional mode of winter SIC variability occur in a region of the central GS and show a pattern consistent with a dynamic response of the sea ice drift to the strength of the northerly winds in the EGC. The mechanism, already mentioned in earlier analysis [*Schlichtholz and Houssais*, 2011] implies a modulation of the on-ice/off-ice component of the sea ice drift due to the Ekman drift. Proving that this process is indeed the one at work would require a correlation analysis based on ice drift data. Unfortunately, sea ice drift retrieved from passive microwave observations are often unreliable in this region. Our analysis additionally shows that under northerly winds anomalies the Ekman drift response of the ice should dominate over the opposite effect of the ice efflux through Fram Strait. For instance, under enhanced northerlies, more ice would be advected into the GS at the same time as the ice would be drifting more westward, freeing out the outer GS MIZ.

[38] A weak anticorrelation (−0.41) of the leading mode of GS SIC variability was found with the in-phase PCA-based NAO index [*Hurrell et al.*, 2003]. The correlation becomes insignificant (−0.28) when the NAO leads by 1 year, in contrast with *Kvingedal* [2005a] who obtained a stronger correlation of the mean GS winter sea ice area with the NAO when the latter leads by one year. The difference might come from the different periods used in the two analyses since *Kvingedal* [2005a] analysis is based on an earlier period mostly extending prior to the eastward shift of the northern center of action of the NAO [*Hilmer and Jung*, 2000; *Zhang et al.*, 2008]. Our analysis also shows that the relationship between the GS SIC and the atmosphere is better described within the nonlinear paradigm of atmospheric weather regimes. A composite analysis based on distinct NAO^+ and NAO^- North Atlantic SLP weather regimes indeed indicates asymmetric responses of the SIC to the two phases of the NAO with a preferential response to its negative phase. By contrast, the NAO^+ composite shows a dipolar structure which has some resemblance to the Odden/Nordbukta feature. Consistently, the SIC PC1 may not correlate with the Fram Strait ice efflux partly because it is more sensitive to the NAO^- SLP regimes which are less conducive of changes in the Fram Strait ice efflux than the NAO^+ regimes [*Kwok et al.*, 2004]. On the other hand, the Odden/Nordbukta mode of variability, as depicted by the third mode of the GS winter SIC variability, shows some positive correlation with the Fram Strait ice efflux which could be a manifestation of the better correlation of this efflux with the NAO during the recent period [*Kwok et al.*, 2004].

[39] The statistical link between the SAT and SIC anomalies in the GS is consistent with a possible contribution of the surface atmosphere to sea ice melting/freezing but this mechanism could not be identified unambiguously due to the dominant heat flux feedback of the SIC on the SAT. Several studies have emphasized a possible link between the SAT and the sea ice cover in the Greenland Sea [*Shuchman et al.*, 1998; *Comiso et al.*, 2001]. This relationship was however mainly analyzed in the context of the intraseasonal variability. Here, we analyzed this relationship in the context of winter averaged anomalies and found evidence of a thermal feedback of the sea ice onto the atmosphere via the air-ice heat flux. A similar feedback was also identified by *Schlichtholz and Houssais* [2011] in relation to the interannual variability of the Atlantic Current at the western entrance of the Barents Sea. In the present study, it was not possible to ascertain nor to quantify the direct impact of the SAT on the sea ice as both this forcing and the feedback would lead to SAT anomalies of the same sign. The feedback was also clearly identified in the Nordbukta region but, there, with no signature on the SAT.

[40] The present analysis has focused on the statistical links between the SIC and the surface atmosphere. The exact processes underpinning these links are still to be understood. Beyond the impact of the atmospheric circulation on the sea ice drift and melt/growth many other processes should indeed be investigated in relation to the ocean response to the atmosphere and its feedback on the ice. Ocean convection, through the heat flux associated with vertical mixing bringing warm intermediate water masses to the surface, is believed to play an important role in the Nordbukta development during winter [*Carsey and Roach*, 1994; *Roach et al.*, 1993; *Visbeck et al.*, 1995]. Conversely, the thermal insulation by sea ice as well as brine rejection/fresh water release during ice formation/melting should affect the timing and intensity of the water column homogenization. The statistical link between the sea ice and the convection is however very difficult to establish in view of the lack of relevant indices of convection over a sufficiently long period. In an attempt to quantify this link, we correlated the GS convection index proposed by *Budéus and Ronski* [2009] for the period 1994–2005 with the leading modes of variability of the GS winter SIC (Table 2). No significant correlations are found with either the first or third modes. A significant negative correlation is however identified

with the second mode. The latter is indeed characterized by a dipole of SIC anomalies between the Greenland slope and the convective region (Figure 5c), suggesting a link of the convection activity with the sea ice distribution in the central gyre rather than with the overall extent of the sea ice cover. These links should however be taken with caution as this mode of SIC variability was found to reproduce only a small part of the Greenland Sea SIC variance and the time series of convection is based on limited ocean sampling and on an indirect estimate of the strength of the convection [*Germe*, 2011].

[41] The wind patterns identified in relation to the leading modes of GS winter SIC variability have a rotational centered over the Greenland-Icelandic Sea which may have consequences on the strength of the cyclonic Greenland Gyre as well as on the heat and fresh water transport [*Jonsson*, 1991; *Dickson et al.*, 1996]. A collapse of the isopycnal dome in response to a decrease of the wind stress curl over the Greenland Sea would enhance the eastward expansion of sea ice and fresh polar water into the GS [*Meincke et al.*, 1992; *Malmberg and Jonsson*, 1997] thus possibly affecting local ice formation and melting. All these links need to be better understood in order to get a full understanding of the GS sea ice cover variability.

[42] **Acknowledgments.** The authors would like to thank Chantal Claud and Gilles Reverdin for stimulating discussions and Pawel Schichtholz for his helpful comments on the manuscript. The authors are also grateful to Sophie Cloché for extracting the ERA Interim reanalysis surface fields and to Ron Kwok for providing the time series of annual ice area flux through Fram Strait over the 1979–2007 period. The above research has received funding from the French Direction Générale de l'Armement (DGA) and from the European Community 7th Framework Programme through the THOR (Thermohaline Overturning – at Risk) project (2008–2012) under Grant agreement GA212643. The main author is also grateful to Juliette Mignot for enlightening discussions on statistics.

References

Berrisford, P., D. Dee, K. Fielding, M. Fuentes, P. Kallberg, S. Kobayashi, and S. Uppala (2009), The ERA Interim archive, technical report, Eur. Cent. for Medium-Range Weather Forecasts, Reading, U. K.

Budéus, G., and S. Ronski (2009), An integral view of the hydrographic development in the Greenland Sea over a decade, *Open Oceanogr. J.*, *3*, 8–39, doi:10.2174/1874252100903010008.

Carsey, F. D., and A. T. Roach (1994), Oceanic convection in the Greenland Sea Odden region as interpreted in satellite data, in *The Polar Oceans and Their Role in Shaping the Global Environment*, *Geophys. Monogr. Ser.*, vol. 85, edited by O. M. Johannessen, R. D. Muench, and J. E. Overland, pp. 211–222, AGU, Washington, D. C.

Cassou, C. (2008), Intraseasonal interaction between the Madden-Julian Oscillation and the North Atlantic Oscillation, *Nature*, *455*, 523–527, doi:10.1038/nature07286.

Cassou, C., L. Terray, J. Hurrell, and C. Deser (2004), North Atlantic winter climate regimes: Spatial asymmetry, stationarity with time, and oceanic forcing, *J. Clim.*, *17*, 1055–1068, doi:10.1175/1520-0442(2004)017<1055:NAWCRS>2.0.CO;2.

Cavalieri, D. J., and C. L. Parkinson (1987), On the relationship between atmospheric circulation and the fluctuations in the sea ice extents of the Bering and Okhotsk seas, *J. Geophys. Res.*, *92*, 7141–7162, doi:10.1029/JC092iC07p07141.

Cavalieri, D. J., P. Gloersen, and W. J. Campbell (1984), Determination of sea ice parameters with the Nimbus 7 SMMR, *J. Geophys. Res.*, *89*, 5355–5369, doi:10.1029/JD089iD04p05355.

Cavalieri, D. J., C. L. Parkinson, P. Gloersen, and H. J. Zwally (1996), Sea Ice Concentrations From Nimbus-7 SMMR and DMSP SSM/I Passive Microwave Data, http://nsidc.org/data/nsidc-0051.html, Natl. Snow and Ice Data Cent., Boulder, Colo. [Updated 2008.]

Comiso, J. C. (1986), Characteristics of winter sea ice from satellite multispectral microwave observations, *J. Geophys. Res.*, *91*, 975–994, doi:10.1029/JC091iC01p00975.

Comiso, J. C., P. Wadhams, L. T. Pedersen, and R. A. Gersten (2001), Seasonal and interannual variability of the Odden ice tongue and a study of environmental effects, *J. Geophys. Res.*, *106*, 9093–9116, doi:10.1029/2000JC000204.

Deser, C., J. E. Walsh, and M. S. Timlin (2000), Arctic sea ice variability in the context of recent atmospheric circulation trends, *J. Clim.*, *13*, 617–633, doi:10.1175/1520-0442(2000)013<0617:ASIVIT>2.0.CO;2.

Dickson, R., J. Lazier, J. Meincke, P. Rhines, and J. Swift (1996), Long-term coordinated changes in the convective activity of the North Atlantic, *Prog. Oceanogr.*, *38*, 241–295, doi:10.1016/S0079-6611(97)00002-5.

Fang, Z., and J. M. Wallace (1994), Arctic sea ice variability on a timescale of weeks and its relation to atmospheric forcing, *J. Clim.*, *7*, 1897–1914, doi:10.1175/1520-0442(1994)007<1897:ASIVOA>2.0.CO;2.

Germe, A. (2011), Variabilité de la glace de mer en mer du Groenland: Liens avec les forçages atmosphériques et océaniques à l'échelle interannuelle, Ph.D. thesis, Univ. Pierre et Marie Curie, Paris.

Gloersen, P. (1995), Modulation of hemispheric sea-ice cover by ENSO events, *Nature*, *373*, 503–506, doi:10.1038/373503a0.

Gloersen, P., and D. J. Cavalieri (1986), Reduction of weather effects in the calculation of sea ice concentration from microwave radiances, *J. Geophys. Res.*, *91*, 3913–3919, doi:10.1029/JC091iC03p03913.

Gloersen, P., et al. (1984), A summary of results from the first Nimbus 7 SMMR observations, *J. Geophys. Res.*, *89*, 5335–5344, doi:10.1029/JD089iD04p05335.

Hilmer, M., and T. Jung (2000), Evidence for a recent change in the link between the North Atlantic Oscillation and Arctic sea ice export, *Geophys. Res. Lett.*, *27*(7), 989–992, doi:10.1029/1999GL010944.

Hurrell, J., Y. Kushnir, G. Ottersen, and M. Visbeck (2003), An overview of the North Atlantic oscillation, in *The North Atlantic Oscillation: Climatic Significance and Environmental Impact*, *Geophys. Monogr. Ser.*, vol. 134, edited by J. W. Hurrell et al., pp. 1–36, AGU, Washington, D. C.

Jonsson, S. (1991), Seasonal and interannual variability of wind stress curl over the Nordic Seas, *J. Geophys. Res.*, *96*, 2649–2659, doi:10.1029/90JC02230.

Kern, S., L. Kaleschke, and G. Spreen (2010), Climatology of the Nordic (Irminger, Greenland, Barents, Kara and White Pechora) Seas ice cover based on 85 GHz satellite microwave radiometry: 1992–2008, *Tellus, Ser. A*, *62*, 411–434, doi:10.1111/j.1600-0870.2010.00457.x.

Kvingedal, B. (2005a), On sea ice variability in the Nordic Seas, Ph.D. thesis, Univ. of Bergen, Bergen, Germany.

Kvingedal, B. (2005b), Sea-ice extent and variability in the Nordic Seas, 1967–2002, in *The Nordic Seas: An Integrated Perspective Oceanography, Climatology, Biogeochemistry, and Modeling*, *Geophys. Monogr. Ser.*, vol. 158, edited by H. Drange et al., pp. 39–49, AGU, Washington, D. C.

Kwok, R. (2009), Outflow of Arctic Ocean sea ice into the Greenland and Barents seas: 1979–2007, *J. Clim.*, *22*, 2438–2457, doi:10.1175/2008JCLI2819.1.

Kwok, R., and D. A. Rothrock (1999), Variability of Fram Strait ice flux and North Atlantic Oscillation, *J. Geophys. Res.*, *104*, 5177–5189, doi:10.1029/1998JC900103.

Kwok, R., G. F. Cunningham, and S. S. Pang (2004), Fram Strait sea ice outflow, *J. Geophys. Res.*, *109*, C01009, doi:10.1029/2003JC001785.

Malmberg, S.-A., and S. Jonsson (1997), Timing of deep convection in the Greenland and Iceland seas, *ICES J. Mar. Sci.*, *54*, 300–309, doi:10.1006/jmsc.1997.0221.

Meincke, J., J. Jonsson, and J. Swift (1992), Variability of convective conditions in the Greenland Sea, *ICES Mar. Sci. Symp.*, *195*, 32–39.

Michelangeli, P.-A., R. Vautard, and B. Legras (1995), Weather regimes: Recurrence and quasi stationarity, *J. Atmos. Sci.*, *52*, 1237–1256, doi:10.1175/1520-0469(1995)052<1237:WRRAQS>2.0.CO;2.

Mysak, L. A., and D. K. Manak (1989), Arctic sea-ice extent and anomalies, 1953–1984, *Atmos. Ocean*, *27*, 376–405, doi:10.1080/07055900.1989.9649342.

Mysak, L. A., and S. A. Venegas (1998), Decadal climate oscillations in the Arctic: A new feedback loop for atmosphere-ice-ocean interactions, *Geophys. Res. Lett.*, *25*, 3607–3610, doi:10.1029/98GL02782.

North, G. R., T. L. Bell, R. F. Cahalan, and F. J. Moeng (1982), Sampling errors in the estimation of empirical orthogonal functions, *Mon. Weather Rev.*, *110*, 699–706, doi:10.1175/1520-0493(1982)110<0699:SEITEO>2.0.CO;2.

Parkinson, C. L., D. J. Cavalieri, P. Gloersen, H. J. Zwally, and J. C. Comiso (1999), Arctic sea ice extents, area, and trends, 1978–1996, *J. Geophys. Res.*, *104*, 20,837–20,856, doi:10.1029/1999JC900082.

Partington, K., T. Flynn, D. Lamb, C. Bertoia, and K. Dedrick (2003), Late twentieth century Northern Hemisphere sea-ice record from U.S. National Ice Center ice charts, *J. Geophys. Res.*, *108*(C11), 3343, doi:10.1029/2002JC001623.

Reinhold, B. B., and R. T. Pierrehumbert (1982), Dynamics of weather regimes—Quasi-stationary waves and blocking, *Mon. Weather Rev.*, *110*, 1105–1145, doi:10.1175/1520-0493(1982)110<1105:DOWRQS>2.0.CO;2.

Reynolds, R. W., N. A. Rayner, T. M. Smith, D. C. Stokes, and W. Wang (2002), An improved in situ and satellite SST analysis for climate, *J. Clim.*, *15*, 1609–1625, doi:10.1175/1520-0442(2002)015<1609:AIISAS>2.0.CO;2.

Roach, A. T., K. Aagaard, and F. Carsey (1993), Coupled ice-ocean variability in the Greenland Sea, *Atmos.-Ocean*, *31*, 319–337, doi:10.1080/07055900.1993.9649474.

Rogers, J. C., and M.-P. Hung (2008), The Odden ice feature of the Greenland Sea and its association with atmospheric pressure, wind, and surface flux variability from reanalyses, *Geophys. Res. Lett.*, *35*, L08504, doi:10.1029/2007GL032938.

Schlichtholz, P., and M.-N. Houssais (2011), Forcing of oceanic heat anomalies by air-sea interactions in the Nordic Seas area, *J. Geophys. Res.*, *116*, C01006, doi:10.1029/2009JC005944.

Shuchman, R. A., E. G. Josberger, C. A. Russel, K. W. Fischer, O. M. Johannessen, J. Johannessen, and P. Gloersen (1998), Greenland Sea Odden sea ice feature: Intra-annual and interannual variability, *J. Geophys. Res.*, *103*, 12,709–12,724, doi:10.1029/98JC00375.

Singarayer, J. S., and J. L. Bamber (2003), EOF analysis of three records of sea-ice concentration spanning the last 30 years, *Geophys. Res. Lett.*, *30*(5), 1251, doi:10.1029/2002GL016640.

Steele, M., R. Morley, and W. Ermold (2001), PHC: A global ocean hydrography with a high quality Arctic Ocean, *J. Clim.*, *14*, 2079–2087, doi:10.1175/1520-0442(2001)014<2079:PAGOHW>2.0.CO;2.

Swift, J. (1986), The arctic waters, in *The Nordic Seas*, edited by B. G. Hurdle, pp. 129–153, Springer, New York.

Tsukernik, M., C. Deser, M. Alexander, and R. Thomas (2009), Atmospheric forcing of Fram strait sea ice export: A closer look, *Clim. Dyn.*, *35*(7–8), 1349–1360.

Ukita, J., M. Honda, H. Nakamura, Y. Tachibana, D. J. Cavalieri, C. L. Parkinson, H. Koide, and K. Yamamoto (2007), Northern Hemisphere sea ice variability: Lag structure and its implications, *Tellus, Ser. A*, *59*, 261–272, doi:10.1111/j.1600-0870.2006.00223.x.

Uppala, S. M., et al. (2005), The ERA-40 re-analysis, *Q. J. R. Meteorol. Soc.*, *131*, 2961–3012, doi:10.1256/qj.04.176.

Vautard, R. (1990), Multiple weather regimes over the North Atlantic analysis of precursors and successors, *Mon. Weather Rev.*, *118*(10), 2056–2081, doi:10.1175/1520-0493(1990)118<2056:MWROTN>2.0.CO;2.

Vinje, T. (2001a), Anomalies and trends of sea-ice extent and atmospheric circulation in the Nordic Seas during the period 1864–1998, *J. Clim.*, *14*, 255–267, doi:10.1175/1520-0442(2001)014<0255:AATOSI>2.0.CO;2.

Vinje, T. (2001b), Fram Strait ice fluxes and atmospheric circulation: 1950–2000, *J. Clim.*, *14*, 3508–3517, doi:10.1175/1520-0442(2001)014<3508:FSIFAA>2.0.CO;2.

Visbeck, M., J. Fischer, and F. Schott (1995), Preconditioning the Greenland Sea for deep convection: Ice formation and ice drift, *J. Geophys. Res.*, *100*, 18,489–18,502, doi:10.1029/95JC01611.

Wadhams, P., and J. C. Comiso (1999), Two modes of appearance of the Odden ice tongue in the Greenland Sea, *Geophys. Res. Lett.*, *26*, 2497–2500, doi:10.1029/1999GL900502.

Wadhams, P., J. C. Comiso, E. Prussen, S. Wells, M. Brandon, E. Aldworth, T. Viehoff, R. Allegrino, and D. R. Crane (1996), The development of the Odden ice tongue in the Greenland Sea during winter 1993 from remote sensing and field observations, *J. Geophys. Res.*, *101*, 18,213–18,235, doi:10.1029/96JC01440.

Walsh, J. E., and C. M. Johnson (1979), An analysis of Arctic sea ice fluctuations, 1953–77, *J. Phys. Oceanogr.*, *9*, 580–591, doi:10.1175/1520-0485(1979)009<0580:AAOASI>2.0.CO;2.

Zhang, X., A. Sorteberg, J. Zhang, R. Gerdes, and J. C. Comiso (2008), Recent radical shifts of atmospheric circulations and rapid changes in Arctic climate system, *Geophys. Res. Lett.*, *35*, L22701, doi:10.1029/2008GL035607.

C. Cassou, Climate Modelling and Global Change Project, CNRS-CERFACS, 42 ave. G. Coriolis, Toulouse F-31057, France.

A. Germe, C. Herbaut, and M.-N. Houssais, LOCEAN, UMR 7159, CNRS/UPMC/IRD/MNHN, 4 place Jussieu, Paris F-75252 CEDEX 05, France. (mnh@locean-ipsl.upmc.fr)